Am J Cancer Res 2020;10(5):1384-1399
www.ajcr.us /ISSN:2156-6976/ajcr0108592

Original Article

Inhibiting ULK1 kinase decreases autophagy and cell viability in high-grade serous ovarian cancer spheroids

Bipradeb Singha[1,2], Jeremi Laski[1,2], Yudith Ramos Valdés[1], Elaine Liu[1], Gabriel E DiMattia[1,3,5], Trevor G Shepherd[1,2,4,5]

[1]The Mary & John Knight Translational Ovarian Cancer Research Unit, London Regional Cancer Program, London, Ontario, Canada; Departments of [2]Anatomy & Cell Biology, [3]Biochemistry, [4]Obstetrics & Gynaecology, Schulich School of Medicine and Dentistry, Western University, London, Ontario, Canada; [5]Department of Oncology, Schulich School of Medicine and Dentistry, The University of Western Ontario, London, Ontario, Canada

Received February 1, 2020; Accepted February 27, 2020; Epub May 1, 2020; Published May 15, 2020

Abstract: Metastasis in high-grade serous ovarian cancer (HGSOC) occurs through an unconventional route that involves exfoliation of cancer cells from primary tumors and peritoneal dissemination via multicellular clusters or spheroids. Previously, we demonstrated autophagy induction in HGSOC spheroids grown *in vitro* and in spheroids collected from ovarian cancer patient ascites; thus, we speculate that autophagy may contribute to spheroid cell survival and overall disease progression. Hence, in this study we sought to evaluate whether ULK1 (unc-51-like kinase-1), a serine-threonine kinase critical for stress-induced autophagy, is important for autophagy regulation in HGSOC spheroids. We demonstrate that HGSOC spheroids have increased ULK1 protein expression that parallels autophagy activation. *ULK1* knockdown increased p62 accumulation and decreased LC3-II/I ratio in HGSOC spheroids. In addition, knocking down ATG13, a protein that regulates ULK1 activity via complex formation, phenocopied our ULK1 knockdown results. HGSOC spheroids were blocked in autophagic flux due to *ULK1* and *ATG13* knockdown as determined by an mCherry-eGFP-LC3B fluorescence reporter. These observations were recapitulated when HGSOC spheroids were treated with an ULK1 kinase inhibitor, MRT68921. Autophagy regulation in normal human fallopian tube epithelial FT190 cells, however, may bypass ULK1, since MRT68921 reduced viability in HGSOC spheroids but not in FT190 cells. Interestingly, *ULK1* mRNA expression is negatively correlated with patient survival among stage III and stage IV serous ovarian cancer patients. As we observed using established HGSOC cell lines, cultured spheroids using our new, patient-derived HGSOC cells were also sensitive to ULK1 inhibition and demonstrated reduced cell viability to MRT68921 treatment. These results demonstrate the importance of ULK1 for autophagy induction in HGSOC spheroids and therefore justifies further evaluation of MRT68921, and other novel ULK1 inhibitors, as potential therapeutics against metastatic HGSOC.

Keywords: Autophagy, high-grade serous ovarian cancer, spheroids, ULK1, MRT68921

Introduction

Most women with high-grade serous ovarian cancer (HGSOC) are first diagnosed with late-stage disease, thus contributing to poor prognosis and increased lethality. While patients initially respond to treatment that includes both cytoreductive surgery and chemotherapy, most patients relapse with chemoresistant disease. Hence, understanding the mechanisms that promote metastasis and disease recurrence is critical for improving treatment outcomes among HGSOC patients. One of the hallmarks of HGSOC metastasis lies in the process of cancer cells exfoliating from primary tumors and forming multicellular clusters called spheroids. By forming spheroids, detached cancer cells have an enhanced capacity to survive anoikis, nutrient deprivation, and chemotherapy, and induce cellular quiescence thereby maintaining a state of tumor dormancy. Moreover, spheroids may promote metastasis through increased ability to adhere and invade serosal surfaces of the peritoneal cavity [1-3].

Macroautophagy (herein referred to as autophagy) is a crucial intracellular degradation system that is utilized by cells to survive unfavorable growth conditions [4]. However, cancer cells can exploit autophagy to survive hypoxic

and nutrient-deprived conditions to potentiate overall disease progression [5]. Previously, we demonstrated that HGSOC spheroids actively induce autophagy [6], which we speculate contributes to the survival of cancer cells within spheroids thereby facilitating disease progression. Thus, deciphering the mechanisms of autophagy regulation and determining novel strategies to block autophagy in HGSOC spheroids may prevent metastasis, cancer recurrence and chemoresistance.

The serine-threonine kinase uncoordinated 51-like kinase 1 (ULK1) is a component of the autophagy initiation complex in mammalian cells that initiates autophagy following stress. Although ULK1 is known to initiate autophagy in mammalian cells following stress, the mechanism of autophagy regulation and involvement of ULK1 can be highly contextual and variable [7, 10-18]. Under stressed conditions, ULK1 activation relies on phosphorylation by AMPK that blocks mTORC1 mediated ULK1 inhibition [7]. We have seen previously that HGSOC spheroids exhibit activation of AMPK [8] along with downregulation of the AKT-mTORC1 pathway [9]. These observations indicate a possible role for ULK1 activation during autophagy induction in HGSOC spheroids. Therefore, we sought to elucidate whether ULK1 is required for autophagy induction in HGSOC spheroids, and whether this kinase can be targeted using pharmacological inhibitors as a potential novel therapy against metastatic HGSOC.

Herein, we show that HGSOC spheroids have elevated ULK1 expression that parallels activated autophagy as compared with adherent monolayer cells. ULK1 loss increased p62 accumulation, decreased LC3-II/I ratio, and reduced autophagic flux in HGSOC spheroids. Furthermore, we provide the first evidence of successfully targeting ULK1 using the pharmacological inhibitor MRT68921 in HGSOC spheroids. ULK1 inhibition through MRT68921 treatment blocked autophagy induction and decreased cell viability in HGSOC spheroids. Additionally, since high *ULK1* mRNA expression has a negative correlation with survival outcomes among advanced-stage serous ovarian cancer patients, we propose that targeting ULK1 may improve treatment outcomes and arrest disease progression among HGSOC patients.

Materials and methods

Cell culture

OVCAR3, OVCAR4 (gifts from J. Koropatnick, Western University) and OVCAR8 cells (ATCC) were cultured in RPMI-1640 (Wisent) supplemented with 10% fetal bovine serum (FBS). COV318, COV362 (gifts from Z. Khan, Western University), CaOV3 (ATCC) and FT190 cells (gift from R. Drapkin, University of Pennsylvania) were grown in DMEM/F12 supplemented with 10% FBS. Patient-derived ovarian cancer cell lines (iOvCa147, iOvCa256, and iOvCa360) were generated from primary cultures of ascites-derived cells collected at the time of surgery or paracentesis to establish immortalized lines. Patient consent for all clinical specimens was obtained according to our institutional human studies research ethics board approved protocol. These three cell lines represent high-grade serous cancer based upon pathology reports of the primary tumors, and they have been verified for mutant *TP53* status and copy number alterations by OncoPanel and Illumina SNP arrays (SickKids Hospital, Toronto, ON, Canada), respectively. iOvCa cell lines were grown in DMEM/F12 supplemented with 10% FBS. All cell lines used in this study have been verified by STR analysis (SickKids Hospital, Toronto, ON, Canada) and confirmed negative for mycoplasma (ATCC, 30-1012K). For monolayer cultures, cells were seeded at a density of 1.0×10^5 cells/well of a tissue culture-treated 6-well plate. For spheroid cultures, cells were seeded at a density of 3.0×10^5 cells/well of a 6-well Ultra-Low Attachment (ULA) plate, or 1.0×10^5 cells/well of a 24-well ULA plate.

siRNA transfection

Cells were seeded at a density of 1.0×10^5 cells/well on tissue culture-treated 6-well plates and the following day transfection was performed using DharmaFECT1 according to the manufacturer's protocol (Dharmacon, Waltham, MA). Briefly, 1 µl of DharmaFECT1 was combined with 10 nM siRNA in 1 ml serum-free media for transfection. After 24 hours, media was replaced with complete growth media and cells were incubated for 48 hours. For obtaining knockdown spheroids, the siRNA-transfected cells were harvested and reseeded at a density of 1.0×10^5 cells/well of a 24-well

ULA plate; protein lysates were harvested after 72 hours in spheroid culture.

Western blot

Protein lysates (20 μg) were resolved on either a 10% or 12% polyacrylamide/SDS gel then transferred to Immobilon-P membranes (Millipore). The membranes were blocked using 5% bovine serum albumin (BSA)/Tris-buffered saline-Tween 20 (TBST) and incubated overnight with antibodies against ULK1 (Cell Signaling; 8054S), p62 (Cell Signaling; 5114S), ATG13 (Cell Signaling; 13468S), LC3B (Cell Signaling; 3868S), p-ATG4b (gift from R. Ketteler, University College London), ATG4b (Cell Signaling 5299S) or tubulin (Sigma; 8328). Membranes were subsequently incubated with horseradish peroxidase-conjugated secondary antibody (anti-rabbit: NA934V; anti-mouse: NA931V; GE Healthcare). Luminata Forte ECL reagent (Millipore) and resultant chemiluminescence was detected using the Biorad Chemidoc detection system. ImageJ software was used to quantify protein band intensities.

Reporter cell line generation

OVCAR8 cells were transfected with a reporter construct that expressed mCherry-eGFP-LC3B (pBABE-puro mCherry-eGFP-LC3B, Addgene #22418; gift from Dr. Jayanta Debnath, UCSF, CA). After puromycin selection for positive transfection, eGFP-positive OVCAR8 cells were visualized by microscopy and eGFP-positive colonies were picked and expanded. For COV318 reporter line generation, cells were transfected with the mCherry-eGFP-LC3B reporter, subjected to puromycin selection and surviving cell populations were harvested and expanded.

MRT68921 treatment

MRT68921 (Selleckchem; 2.5 mM in DMSO) was aliquoted and stored at -20°C. Spheroid cells were treated with MRT68921 at the time of seeding on ULA plates using concentrations indicated in the text, and treatment continued for 72 hours.

Spheroid viability assessment

Cells were seeded at a density of 1.0×10^5 cells/well of a 24-well ULA plate with 1 ml complete media. Spheroids were imaged by phase contrast and fluorescence microscopy using a Leica DMI4000B inverted microscope and Leica Application Suite V4 software, then harvested by low-speed centrifugation. After aspiration of media supernatant, spheroids were resuspended in 0.25% Trypsin/EDTA (Wisent) and incubated at 37°C until no cellular clusters were visible. Following neutralization of trypsin with complete growth media, 0.4% Trypan Blue Stain (Gibco) was added, and live/dead cells were quantified using a TC10 Automated Cell Counter (Biorad).

Statistical analysis

Statistical analysis was performed using GraphPad Prism 6 software (GraphPad Software, La Jolla, CA). A *p*-value less than 0.05 was considered significant for all statistical analyses.

Results

ULK1 protein increases in HGSOC spheroids and correlates with autophagy activation

Following exfoliation from the primary tumor, HGSOC cells rely on spheroid formation for surviving anoikis and effective peritoneal dissemination [1-3]. We previously reported that spheroids harvested from patient-derived ascites possess induced autophagy [6], which we speculate contributes to anoikis survival and ovarian cancer metastasis. Although several previous studies have demonstrated ULK1-mediated autophagy initiation under unfavorable growth conditions [7, 10-14], there are additional reports which argue otherwise [15-18]. Thus, to ascertain whether ULK1 is necessary for autophagy regulation in HGSOC spheroids, we sought to elucidate its protein expression under both monolayer and spheroid culture conditions. For this analysis, we seeded six different established HGSOC cell lines using Ultra-Low Attachment (ULA) plates for spheroid culture, and standard tissue culture-treated plates for adherent monolayer culture. We also used a non-cancerous, immortalized human fallopian tube secretory epithelial cell line, FT190, for comparison. HGSOC spheroids exhibited a 3-fold increase in ULK1 protein expression, a result that is consistent with a recent study demonstrating increased *ULK1* gene expression in ovarian cancer cells when cultured in suspension [19]. In concert with increased ULK1, we observed a significant 6-fold increase in LC3-II/I ratio in HGSOC spheroids (**Figure 1A** and **1C**), indicating autophagy induction that

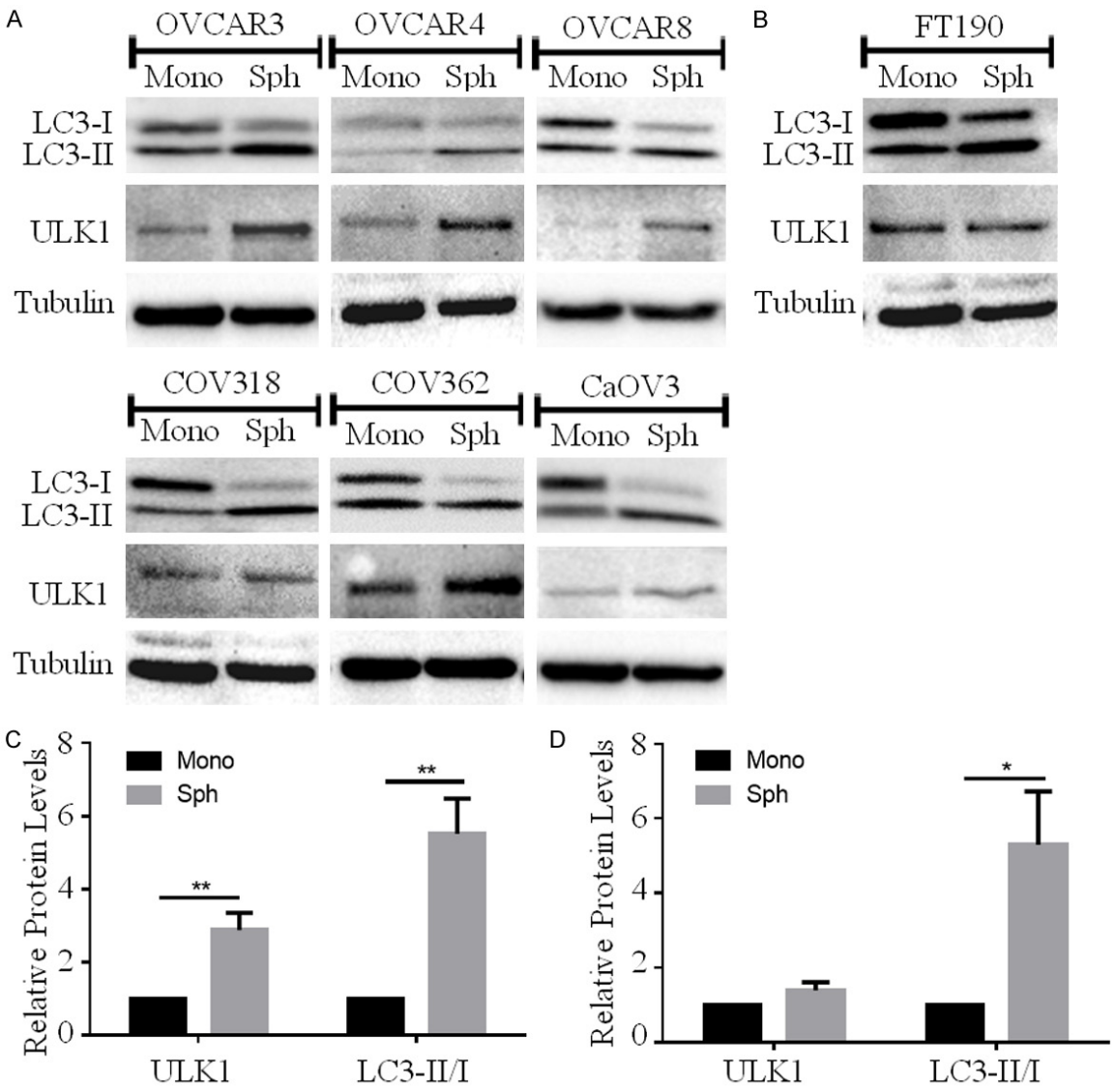

Figure 1. ULK1 protein increases in HGSOC spheroids and correlates with autophagy activation. A. HGSOC cell lines (OVCAR3, OVCAR4, OVCAR8, COV318, COV362 and CaOV3) were seeded for monolayer (Mono) or spheroid (Sph) culture. Protein lysates were harvested 72 h after seeding for western blot analysis to detect ULK1 and LC3B; tubulin served as a loading control. B. Normal human FT190 cells were seeded for monolayer (Mono) or spheroid (Sph) culture and western blot was performed to detect ULK1 and LC3B, with tubulin serving as a loading control. C. Densitometric analysis of ULK1 and LC3-II/I ratio among HGSOC spheroids (n=6) relative to expression in monolayer culture set to 1. Data displayed as mean ± SEM; Student's *t*-test, **P<0.01. D. Densitometric analysis of ULK1 and LC3-II/I ratio in FT190 spheroids (n=3) relative monolayer. Data displayed as mean ± SEM; Student's *t*-test *P<0.05.

follows with our previous results [6]. FT190 spheroids exhibited a 6-fold increase in LC3-II/I ratio as compared with monolayer cells; however, ULK1 protein levels were unaltered (**Figure 1B** and **1D**).

ULK1 knockdown decreases autophagic flux in HGSOC spheroids

Since HGSOC spheroids possessed a coordinate increase in both ULK1 protein expression and autophagy induction, we sought to establish whether ULK1 is necessary for autophagy to occur in HGSOC spheroids. Among all transfected HGSOC cell lines, *ULK1* knockdown was maintained in day-3 spheroids. Interestingly, *ULK1* knockdown increased p62 accumulation yet decreased LC3-II/I ratio (**Figure 2A** and **2C**). ULK1 may be involved in other autophagy-independent cellular functions, such as ER-to-GA vesicular transport and cytokine secretion [20-

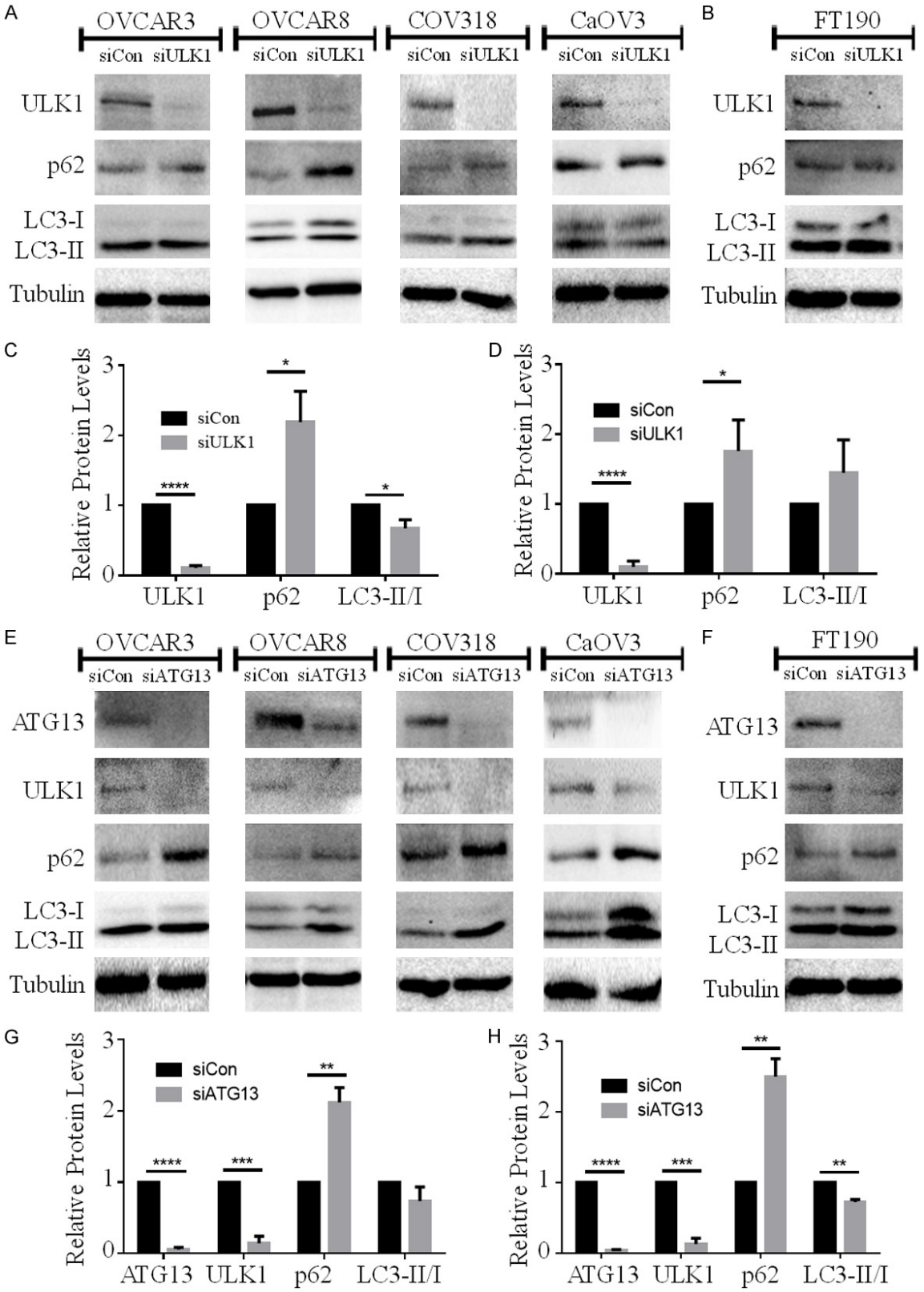

Figure 2. *ULK1* knockdown increases p62 accumulation and decreases LC3-II/I ratio in HGSOC spheroids. A. HGSOC cell lines (OVCAR3, OVCAR8, COV318, CaOV3) were transfected with control siRNA (siCon) or *ULK1* siRNA (siULK1) followed by spheroid culture. Western blot analysis was performed to detect ULK1, p62, and LC3B with tubulin serving as a loading control. B. FT190 cells were transfected with control siRNA (siCon) or *ULK1* siRNA (siULK1) followed by spheroid culture, and subsequent western blot analysis for the indicated proteins. C. Densi-

tometric analysis of ULK1, p62 and LC3-II/I ratio in siULK1-transfected HGSOC spheroids (n=4) relative to siCon spheroids set to 1. Data displayed as mean ± SEM; Student's *t*-test, *P<0.05, ****P<0.0001. D. Densitometric analysis of ULK1, p62 and LC3-II/I ratio in siULK1-transfected FT190 spheroids (n=3) relative to siCon spheroids. Data displayed as mean ± SEM; Student's *t*-test, *P<0.05, ****P<0.0001. E. HGSOC cell lines (OVCAR3, OVCAR8, COV318, CaOV3) were transfected with control siRNA (siCon) or *ATG13* siRNA (siATG13) followed by spheroid culture. Western blot analysis was performed to detect ATG13, ULK1, p62, and LC3B with tubulin serving as a loading control. F. FT190 cells were transfected with control siRNA (siCon) or *ATG13* siRNA (siATG13) followed by spheroid culture, and subsequent western blot analysis for the indicated proteins. G. Densitometric analysis of ATG13, ULK1, p62 and LC3-II/I ratio in siATG13-transfected HGSOC spheroids (n=4) relative to siCon spheroids set to 1. Data displayed as mean ± SEM; Student's *t*-test, **P<0.01, ***P<0.001, ****P<0.0001. H. Densitometric analysis of ATG13, ULK1, p62 and LC3-II/I ratio in siATG13-transfected FT190 spheroids (n=3) relative to siCon spheroids. Data displayed as mean ± SEM; Student's *t*-test, **P<0.01, ***P<0.001, ****P<0.0001.

22]. To further substantiate that our observed changes in p62 and LC3 levels due to *ULK1* knockdown were impacting its role in autophagy, we performed analogous knockdowns targeting ATG13.

ATG13 is an autophagy-related protein within the autophagy initiation complex along with ULK1, and it plays a pivotal role in regulating ULK1 kinase activity through complex formation [23, 24]. Indeed, *ATG13* knockdown resulted in a coordinate and significant decrease in ULK1 protein in HGSOC spheroids. Hence, we hypothesized that *ATG13* knockdown should recapitulate the effects of ULK1 loss on p62 and LC3 levels. Indeed, efficient ATG13 ablation in HGSOC spheroids increased p62 accumulation along with a decrease, albeit non-significant, in the LC3-II/I ratio (**Figure 2E** and **2G**). These data suggest that the result of *ULK1* knockdown on p62 and LC3 levels are most likely through its regulation of autophagy initiation.

In comparison with HGSOC, however, *ULK1* and *ATG13* knockdown had different effects in FT190 spheroids. *ULK1* knockdown increased p62 accumulation, but did not decrease LC3-II/I ratio (**Figure 2B** and **2D**). In contrast, *ATG13* knockdown increased p62 accumulation and decreased LC3-II/I ratio in FT190 spheroids even though ULK1 was still reduced (**Figure 2F** and **2H**), thus suggesting that the mechanisms of autophagy induction in normal FT190 spheroids may bypass ULK1 requirement yet still involve ATG13 function.

Several autophagy independent factors can increase p62 expression [25, 26], and increased LC3-II accumulation on its own may indicate either induction or attenuation of autophagy. Therefore, relying on p62 and LC3 levels to assess the status of autophagy can be misleading. Thus, we sought to address autophagy through a more direct assessment and quantification of autophagic flux.

To investigate the status of autophagic flux in HGSOC spheroids, we stably-transfected OVCAR8 and COV318 cell lines with a reporter plasmid that contained both mCherry and eGFP fused in tandem to LC3 [27]. *ULK1* knockdowns were performed in the OVCAR8 and COV318 reporter cell lines and then seeded to form spheroids. Control siRNA-transfected OVCAR8 reporter spheroids exhibited an abundance of mCherry and low eGFP accumulation, indicating induced autophagic flux (**Figure 3A** and **3B**). *ULK1* knockdown significantly increased both mCherry and eGFP levels in OVCAR8 spheroids (**Figure 3B**) that shifted the overall fluorescence from being predominantly red to yellow in merged images (**Figure 3A**). Although *ULK1* knockdown increased accumulation of both mCherry and eGFP, the mCherry/eGFP ratio was significantly decreased due to ULK1 depletion indicating an early block in autophagic flux (**Figure 3C**). A similar result was observed for *ATG13* knockdown in OVCAR8 mCherry-eGFP-LC3 reporter cell spheroids (**Figure 3A-C**). When repeated in the COV318 reporter cells, both *ULK1* and *ATG13* knockdown increased mCherry and eGFP levels and decreased the mCherry/eGFP ratio (**Figure 3D-F**). Taken together, these data confirm that ULK1 and its complex partner ATG13 are necessary for autophagy induction in HGSOC spheroids.

ULK1 kinase activity is necessary for autophagy regulation in HGSOC spheroids

As a kinase, ULK1 acts to phosphorylate several downstream regulators of autophagy [14]. Since we observed that *ULK1* knockdown blocks autophagy induction in HGSOC spheroids (**Figures 2** and **3**), we sought to evaluate

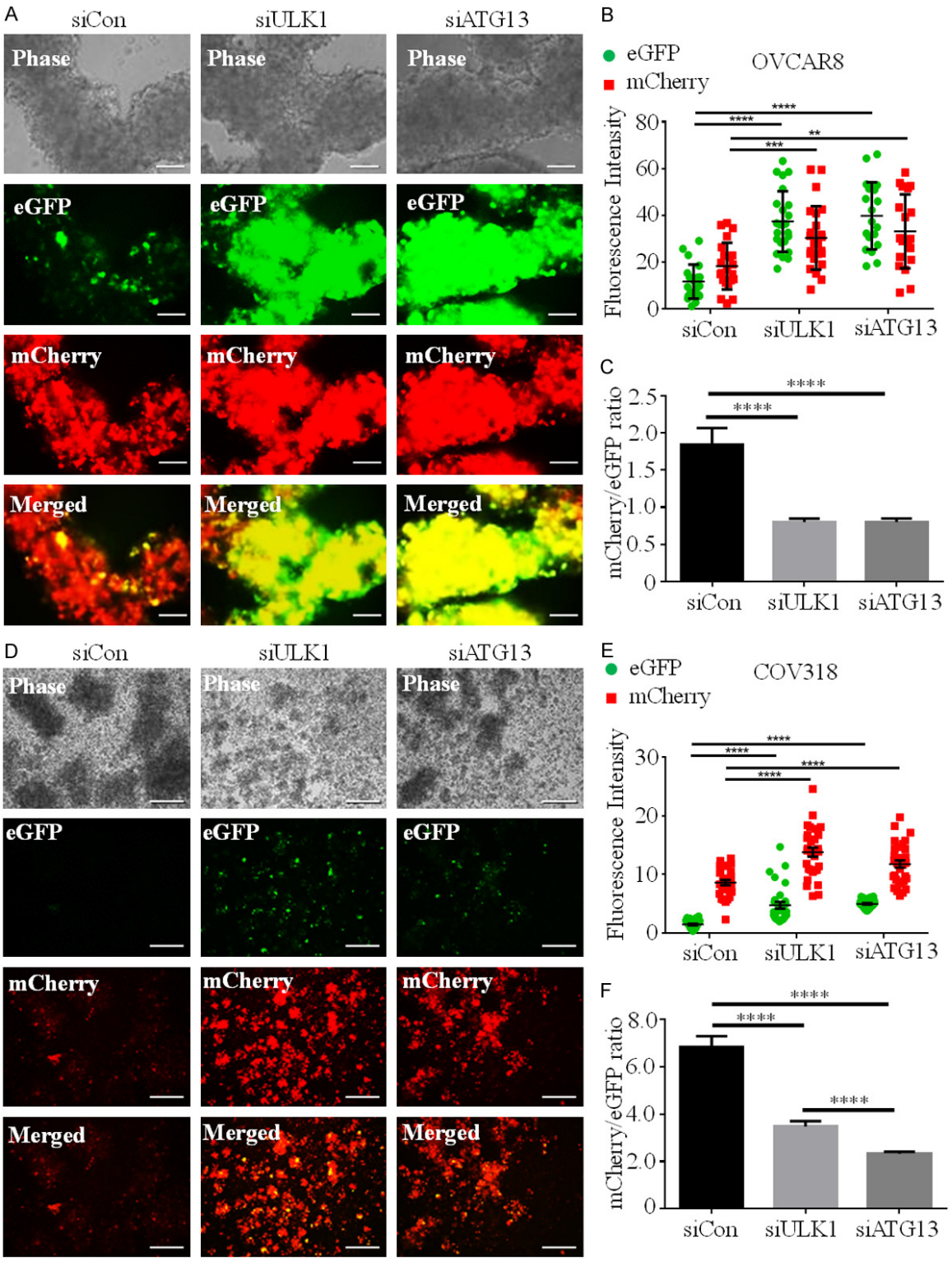

Figure 3. *ULK1* and *ATG13* knockdown blocks autophagic flux in HGSOC spheroids. A. OVCAR8 mCherry-eGFP-LC3B cells were transfected with control (siCon), *ULK1* (siULK1) or *ATG13* (siATG13) siRNA, followed by spheroid culture. Phase contrast and fluorescent images of spheroids were captured at 72 h using a Leica DMI 400B inverted microscope. Scale bars represent 250 μm. B. Fluorescence intensity of eGFP (green) and mCherry (red) in siCon (n=22), siULK1 (n=24) and siATG13 (n=19)-transfected OVCAR8 mCherry-eGFP-LC3B spheroids were quantified using ImageJ. Two-way ANOVA, **P<0.01, ***P<0.001, ****P<0.0001. C. Ratios of mCherry/eGFP in siCon-, siULK1- and siATG13-transfected OVCAR8-mCherry-eGFP-LC3B spheroids are displayed as mean ± SEM; one-way ANOVA, ****P<0.0001. D. COV318-mCherry-eGFP-LC3B cells were transfected with control (siCon), *ULK1* (siULK1)

or *ATG13* (siATG13) siRNA, followed by spheroid culture. Phase contrast and fluorescent images of spheroids were captured at 72 h; scale bars represent 250 μm. E. Fluorescence intensity of eGFP (green) and mCherry (red) in siCon (n=30), siULK1 (n=30) and siATG13 (n=31) transfected COV318 mCherry-eGFP-LC3B spheroids were quantified using ImageJ. Two-way ANOVA, ****P<0.0001. F. Ratios of mCherry/eGFP in siCon-, siULK1- and siATG13-transfected COV318 mCherry-eGFP-LC3B spheroids are displayed as mean ± SEM; one-way ANOVA, ****P<0.0001.

whether its kinase activity is essential for autophagy regulation. To this end, we treated spheroids generated using six different HGSOC cell lines with MRT68921, a recently-described small molecule inhibitor of ULK [28]. We evaluated levels of ATG4b phosphorylation at serine-316 (p-ATG4b) as an indicator of ULK1 kinase activity [29]; MRT68921 treatment consistently decreased p-ATG4b indicating effective inhibition of ULK1 kinase activity (**Figure 4A**). To assess the effects of ULK1 inhibition on autophagy in the HGSOC spheroids, we evaluated p62 expression and LC3-II/I ratio. ULK1 inhibition through MRT68921 treatment increased p62 accumulation and decreased LC3-II/I ratio among HGSOC spheroids (**Figure 4A** and **4C**), which is consistent with our *ULK1* and *ATG13* knockdown data. Interestingly, MRT68921 treatment affected neither p-ATG4b/ATG4b ratio (**Figure 4B**) nor autophagy marker levels (**Figure 4B** and **4D**) in normal FT190 spheroids. These data indicate that MRT68921 can efficiently inhibit ULK1 kinase activity in HGSOC spheroids to block autophagy, yet ULK1 may be dispensable for autophagy induction in normal FT190 spheroids.

To assess ULK1 kinase activity inhibition on autophagic flux, we treated OVCAR8 and COV-318 mCherry-eGFP-LC3 reporter cell line spheroids with or without 5 μM MRT68921 (**Figure 5**). MRT68921 treatment increased eGFP accumulation in the OVCAR8 reporter spheroids (**Figure 5A** and **5B**), which significantly decreased mCherry/eGFP ratio (**Figure 5C**). Similar effects on eGFP levels and mCherry/eGFP ratio were observed when COV318 reporter spheroids were treated with 5 μM MRT68921 (**Figure 5D-F**). Taken together, MRT68921 effectively decreases ULK1 kinase activity to block autophagy induction in HGSOC spheroids.

ULK1 inhibition through MRT68921 treatment decreases cell viability in HGSOC spheroids

Since we speculate that autophagy contributes to cell survival in HGSOC spheroids, we hypothesized that blocking autophagy through ULK1 inhibition would decrease HGSOC spheroid cell viability. MRT68921 treatment occurred for 72 hours during spheroid culture prior to cell viability quantification. All HGSOC spheroids, irrespective of their different spheroid-forming abilities, exhibited a significant reduction in viable cell number due to MRT68921 treatment (**Figure 6**). Moreover, the majority of HGSOC cells failed to form intact spheroid clusters as compared with untreated controls. Interestingly, MRT68921 treatment did not affect cell viability or spheroid formation in FT190 spheroids. These data suggest that blocking autophagy induction through ULK1 inhibition decreases cluster formation and cell viability specifically in HGSOC spheroids.

ULK1 mRNA expression is negatively correlated with patient survival and patient-derived HGSOC spheroids are susceptible to ULK1 inhibition

To evaluate clinical and translational relevance of our study, we sought to decipher whether *ULK1* expression among advanced stage (III and IV) serous ovarian cancer patients is correlated with survival outcomes. Using an online software tool [30], we performed a meta-analysis of datasets obtained from The Cancer Genome Atlas and Gene Expression Omnibus databases to correlate survival outcomes with *ULK1* expression in stage III-IV serous ovarian cancer patients. *ULK1* mRNA expression was associated with decreased overall survival (log rank test, P=0.012) and progression-free survival (log rank test, P=0.00019) (**Figure 7A**). Our results support one recent study which had a smaller dataset and did not focus on advanced-stage HGSOC [19]. To further interrogate translational relevance of therapeutically targeting ULK1, new HGSOC cell lines established from patient-derived ascites were seeded to ULA plates and treated with or without 5 μM MRT68921 for cell viability analysis. As observed with established cell lines, MRT68921 treatment significantly decreased cell viability relative to untreated spheroids across all three patient-derived cell lines, as well as attenuated cell clustering ability (**Figure 7B**). Since high

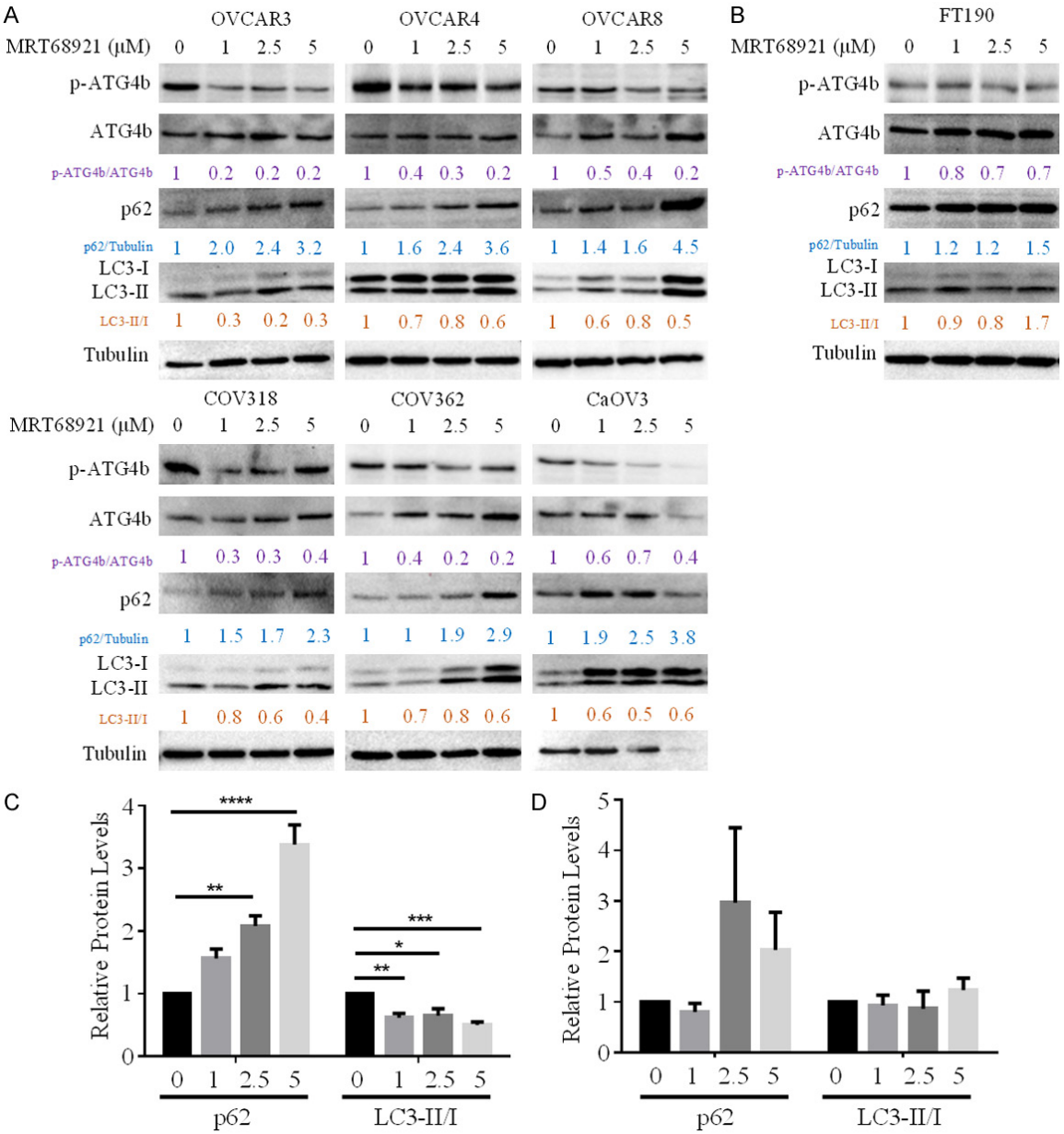

Figure 4. MRT68921 inhibited ULK1 kinase activity, increased p62 levels and decreased LC3-II/I ratio in HGSOC spheroids. A. HGSOC cell lines (OVCAR3, OVCAR4, OVCAR8, COV318, COV362 and CaOV3) were cultured as spheroids and treated with 0, 1, 2.5 and 5 μM MRT68921. Protein lysates were harvested at 72 h for subsequent western blot analysis of p-ATG4b, ATG4b, p62, and LC3B; tubulin served as a loading control. B. FT190 spheroids were treated with 0, 1, 2.5 and 5 μM MRT68921, protein lysates were harvested at 72 h, and western blot analysis was performed for p-ATG4b, ATG4b, p62, and LC3B; tubulin served as a loading control. C. Densitometric analysis of p62 and LC3-II/I ratio in MRT68921-treated HGSOC spheroids (n=6) relative to untreated spheroids set to 1. Data is displayed as mean ± SEM; one-way ANOVA, *P<0.05, **P<0.01, ***P<0.001, ****P<0.0001. D. Densitometric analysis of p62 and LC3-II/I ratio in MRT68921-treated FT190 spheroids (n=3) relative to untreated spheroids set to 1. Data is displayed as mean ± SEM.

ULK1 expression is correlated with poor prognosis among advanced-stage HGSOC patients, then inhibiting ULK1 activity may be beneficial in arresting disease progression and thus result in improved survival outcomes.

Discussion

HGSOC is the most common type of ovarian cancer and is characterized by a high incidence of metastasis and disease recurrence. During

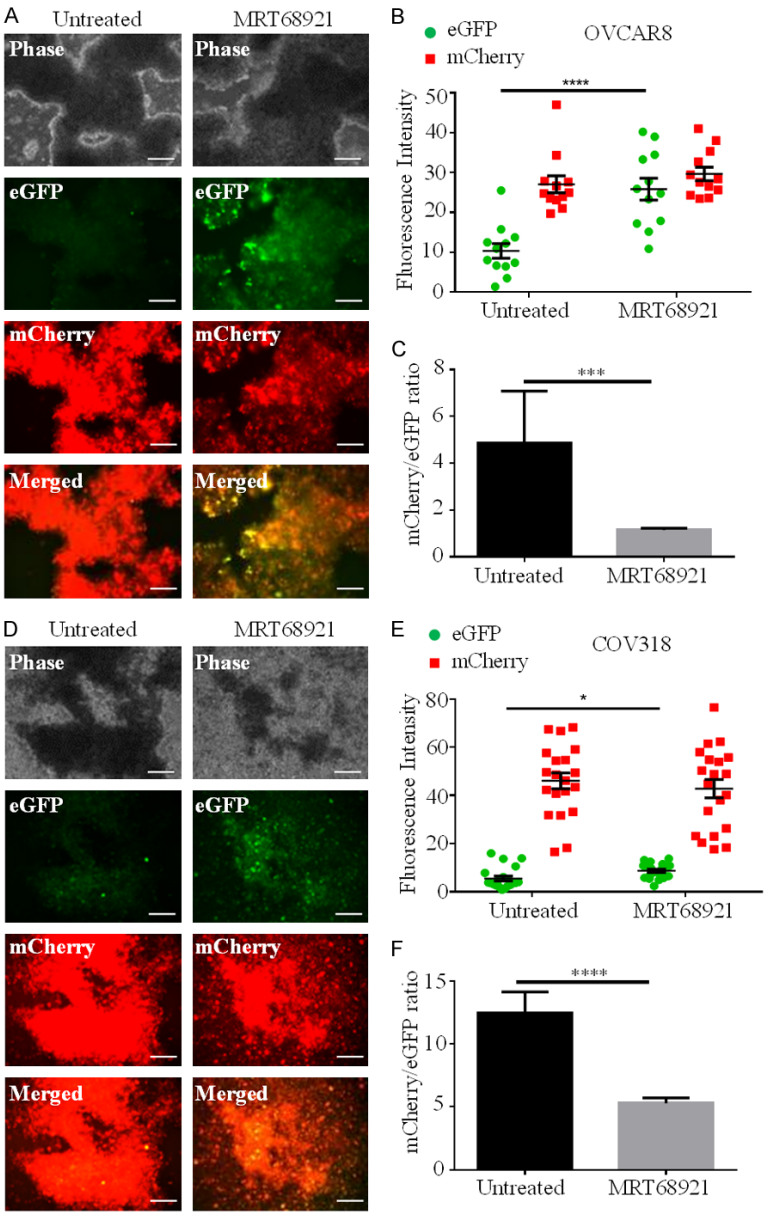

Figure 5. MRT68921 blocks autophagic flux in HGSOC spheroids. A. OVCAR8-mCherry-eGFP-LC3B cells were cultured as spheroids with or without 5 μM MRT68921 for 72 h. Phase contrast and fluorescence images were captured using a Leica DMI 400B inverted microscope. Scale bars represent 250 μm. B. eGFP (green) and mCherry (red) fluorescence intensity in untreated (n=12) and MRT68921-treated (n=12) OVCAR8 mCherry-eGFP-LC3B spheroids was quantified using ImageJ. C. mCherry/eGFP ratios in untreated and MRT68921-treated OVCAR8 mCherry-eGFP-LC3B spheroids are displayed as mean ± SEM; Student's *t*-test, ***P<0.001. D. COV318 mCherry-eGFP-LC3B cells were cultured as spheroids with or without 5 μM MRT68921 for 72 h. Phase contrast and fluorescence images were captured using a Leica DMI 400B inverted microscope. Scale bars represent 250 μm. E. eGFP (green) and mCherry (red) fluorescence intensity in untreated (n=20) and MRT68921-treated (n=20) COV318 mCherry-eGFP-LC3B spheroids was quantified using ImageJ. F. mCherry/eGFP ratios in untreated and MRT68921-treated COV318 mCherry-eGFP-LC3B spheroids are displayed as mean ± SEM; Student's *t*-test, ****P<0.0001.

HGSOC metastasis, cancer cells exfoliate from the primary tumor directly into the peritoneal space where they form multicellular clusters or spheroids. This enables the detached cancer cells to survive anoikis. Furthermore, spheroid formation also facilitates effective dissemination and metastasis through increased invasive capabilities [1-3]. We demonstrated previously that HGSOC spheroids established *in vitro* or harvested from patient-derived ascites have induced autophagy, a crucial result leading us to speculate that autophagy promotes survival of detached cancer cells [6]. Other studies have concurrently reported that autophagy is crucial for maintaining quiescence, survival and tumorigenic potential in ovarian cancer stem-like cells and spheroid cultures [31-33]. Therefore, understanding the mechanisms of autophagy regulation and determining how to inhibit autophagy induction in HGSOC spheroids may prevent cancer cells from surviving anoikis and thereby impede spheroid formation. A common approach to investigate autophagy is performed through depleting key regulators, such as ATG5 or ATG7; however, these regulators are not readily-actionable drug targets. In addition, our previous work revealed that another autophagy regulator Beclin-1 was dispensable for autophagy induction [6]. Therefore, there may be a limited number of druggable targets within the autophagy pathway to block its regulated induction efficiently in HGSOC.

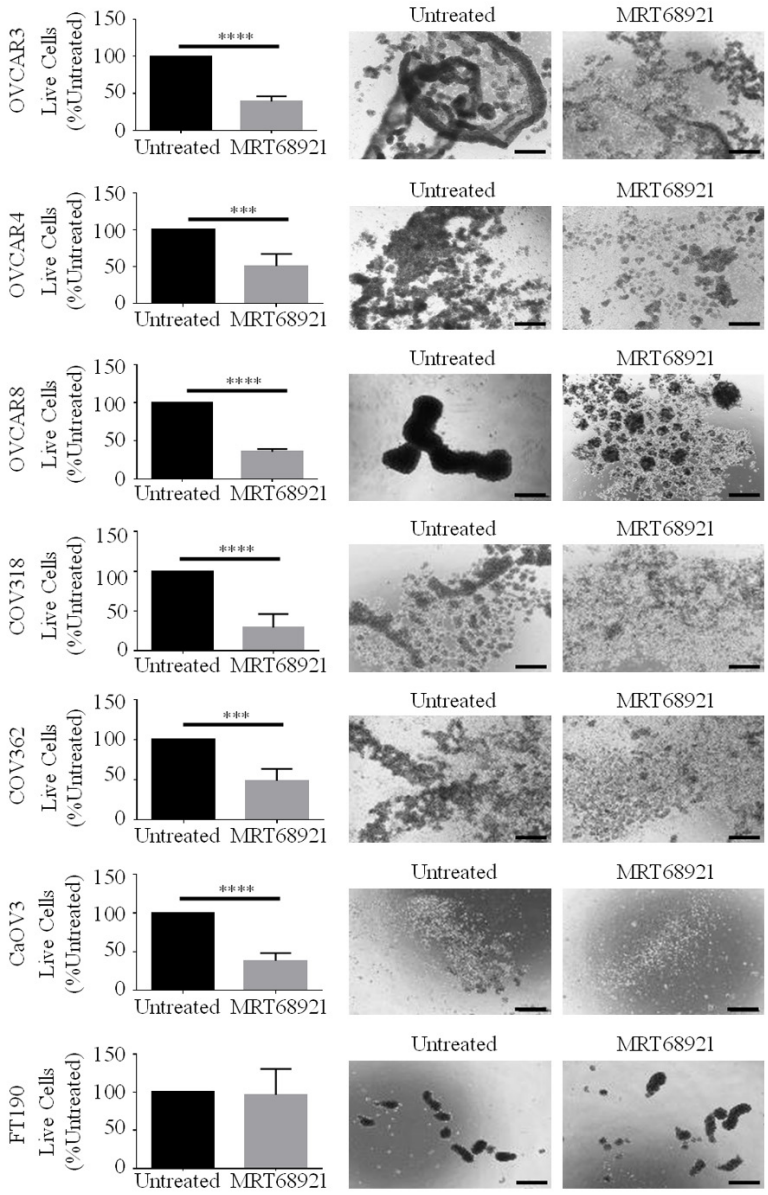

Figure 6. ULK1 inhibition via MRT68921 treatment decreases cell viability in HGSOC spheroids. HGSOC cell lines (OVCAR3, OVCAR4, OVCAR8, COV318, COV362 and CaOV3) and FT190 cells were cultured as spheroids with or without 5 μM MRT68921. Phase contrast images of spheroids were captured after 72 h. Scale bars represent 250 μm. Number of live cells in untreated and MRT68921-treated spheroids were counted using Trypan Blue Exclusion. Data is displayed as mean ± SEM (n=6) percentage of live cells in MRT68921-treated spheroids normalized to untreated spheroids set to 100%. Student's *t*-test, ***P<0.001, ****P<0.0001.

Herein, we demonstrate that ULK1 expression increases in HGSOC spheroids, and *ULK1* knockdown blocks autophagic flux induced in these structures. Similar to our results, a recent study described increased *ULK1* gene expression in ovarian cancer cells cultured in suspension for 48 hours. However, stable *ULK1* knockdown resulted in a modest accumulation of p62 and had no effect on LC3-II/I ratio [19]. In contrast, we observed both an increase in p62 and a decrease in LC3-II/I ratio in *ULK1*-depleted HGSOC spheroids. This discrepancy in results may be explained by duration of suspension culture conditions: Wheeler and colleagues harvested spheroids 48 hours post-seeding [19], whereas we extended this to 72 hours, since this maximizes autophagy induction in HGSOC spheroids (data not shown).

ULK1 is a component of the autophagy initiation complex (AIC) that includes ATG13, FIP200 and ATG101 [34]. ATG13 is crucial for stability of the AIC elements, as *Atg13*$^{-/-}$ MEF cells exhibited reduced levels of ULK1, FIP200 and ATG101 [35]. Similarly, we observed that knocking down *ATG13* in HGSOC spheroids decreases ULK1 protein levels. Therefore, the effects of *ATG13* knockdown on p62 and LC3 processing should recapitulate *ULK1* depletion. Indeed, knocking down *ATG13* and *ULK1* in HGSOC spheroids had nearly identical effects on p62 and LC3 levels. Although monitoring p62 depletion and LC3-II/I ratio is a common way to assess status of autophagy, p62 levels can increase due to autophagy-independent reasons [25, 26]. Furthermore, while increased LC3-II is a hallmark for induced autophagy, it may also indicate blocked clearance of LC3-II due to attenuated autophagy. To address this issue, we stably-transfected HGSOC cell lines with a plasmid that contains LC3 fused to mCherry and eGFP, which is an established approach to visualize and quantify autophagic flux [27]. Using this sys-

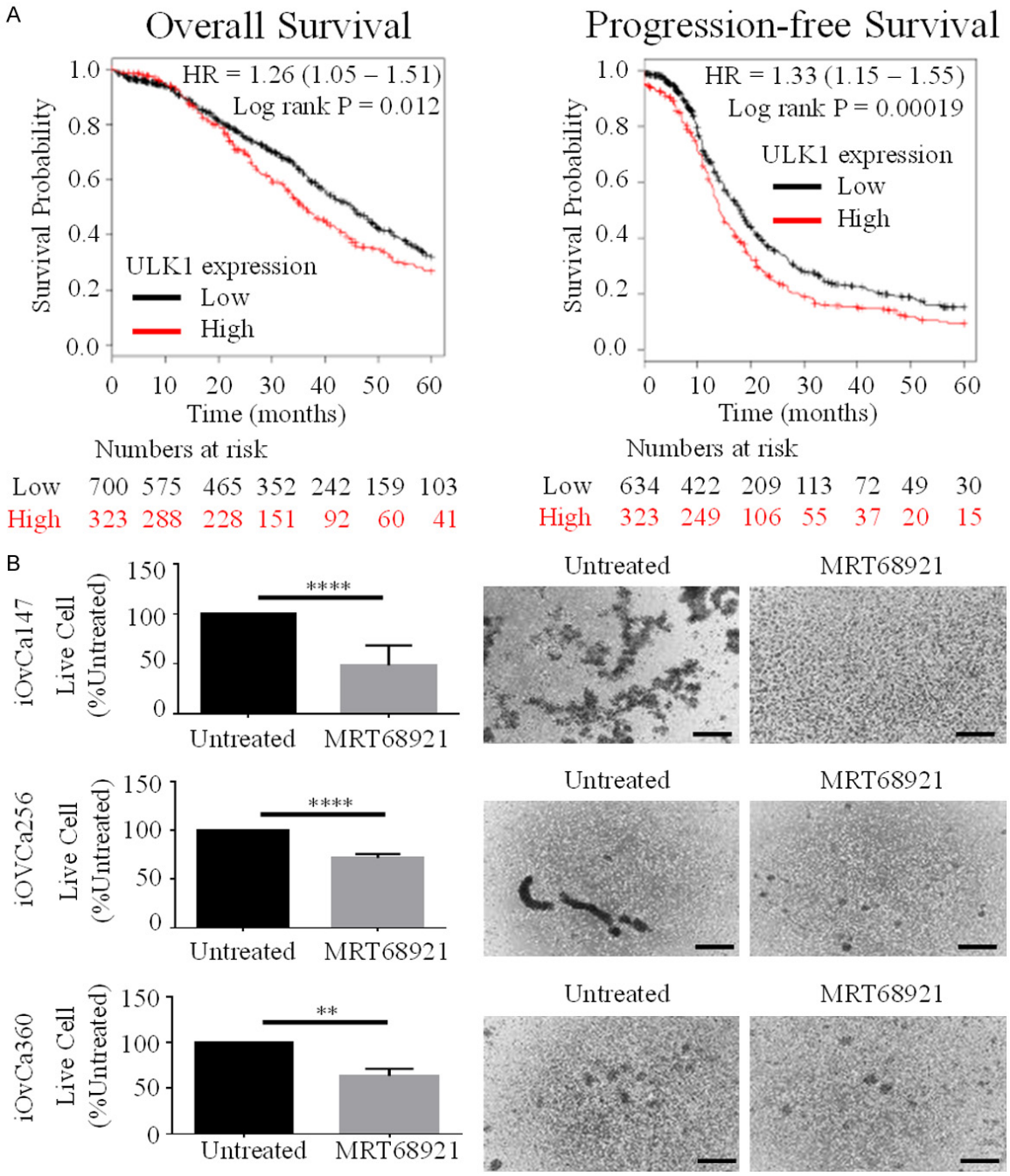

Figure 7. Elevated *ULK1* expression is a negative predictor of patient survival and patient-derived HGSOC spheroids are susceptible to ULK1 inhibition. A. Correlation of low and high *ULK1* expression with overall survival (n=1023) and progression-free survival (n=957) among stage III-IV serous ovarian cancer patients using TCGA and GEO gene expression microarray datasets from the online tool accessed at www.kmplot.com/ovar. Hazard ratios and log rank tests indicate a significantly worse prognosis due to high *ULK1* expression in advanced-stage serous ovarian tumors. B. Three new patient-derived HGSOC cell lines (iOvCa147, iOvCa256, and iOvCa360) were cultured as spheroids with or without 5 μM MRT68921. Phase contrast images were captured at 72 h after seeding; scale bars represent 250 μm. Number of live cells in untreated and MRT68921-treated spheroids were counted using Trypan Blue Exclusion. Data is displayed as mean ± SEM (n=4) percentage of live cells in MRT68921-treated spheroids normalized to untreated spheroids set to 100%. Student's *t*-test, **P,0.01, ****P<0.0001.

tem, we observed that HGSOC spheroids expressing mCherry-eGFP-LC3 are predominantly red. This observation in concert with the observed increase in LC3-II/I ratio confirm that

HGSOC spheroids have autophagy induction. In contrast, HGSOC spheroids with *ULK1* or *ATG13* knockdown had increased eGFP accumulation clearly indicating a block in autophagic flux due to loss of ULK1 or ATG13.

Since ULK1 functions as a serine-threonine kinase [14], and ULK1-induced autophagy has been observed in different cancers [36], several ULK1 kinase inhibitors have been developed in recent years [28, 37, 38]. Herein, we show that a pharmacological inhibitor MRT-68921 can efficiently inhibit kinase activity of ULK1 in HGSOC spheroids, thereby decreasing autophagy induction. Importantly, HGSOC spheroids exhibited consistent sensitivity towards MRT68921 treatment with a significant decrease in cell viability. Although reduced cell viability in ovarian cancer spheroids due to *ULK1* knockdown has been shown recently [19], our data provides the first evidence that ULK1 activity can be targeted therapeutically with a pharmacological inhibitor resulting in the attenuation of both autophagy induction and cell survival in HGSOC spheroids.

In our studies, we used FT190 cells as a non-cancerous control since the distal fallopian tube secretory epithelium is considered to be the precursor site of HGSOC. Interestingly, FT190 spheroids were still able to induce autophagy despite *ULK1* knockdown. In contrast, *ATG13* knockdown increased p62 accumulation and decreased LC3-II/I ratio suggesting that autophagy induction in FT190 spheroids implicates ATG13 but not ULK1. One possibility is that ULK2, a functional homolog of ULK1 [25], is required for autophagy regulation in FT190 spheroids. However, MRT68921 was developed as a potent inhibitor of both ULK1 and ULK2 with IC50 values of 1.1 nM and 2.2 nM, respectively [28]. We demonstrate that MRT68921 treatment neither decreased p-ATG4b levels nor blocked autophagy induction in FT190 spheroids. Although studies report that ULK1 and ULK2 have redundant roles in autophagy regulation, this shared function is not universal. In cerebellar granule neurons, low potassium-induced autophagy is regulated by ULK1, but not by ULK2 [40]. Epithelial-to-mesenchymal transition mediated by autophagy activation in A549 cells is regulated by ULK2 whereas *ULK1* is uninvolved [41]. Finally, another study using DT40 cells demonstrate that an AIC complex lacking both ULK1 and ULK2 may still induce autophagy [16] and expression of an ATG13 variant lacking ULK1/2 binding motifs can partially restore autophagy induction in *Atg13*-null MEFs [42]. These examples provide potential mechanisms of ATG13-dependent autophagy induction in FT190 spheroids without requiring ULK1 or ULK2.

The fact that normal fallopian tube epithelial FT190 cells do not rely on ULK1 for inducing autophagy suggests that targeting ULK1 in HGSOC could provide tumor-specific effects. This idea is supported by observations where ULK1 is not involved in basal autophagy, which may be necessary for normal cellular physiological functions [43]. Therefore, we postulate that targeting ULK1-induced autophagy in metastatic HGSOC may yield tumor-specific effects and overcome the shortcomings of targeting autophagy using chloroquine and its derivatives that affect both pathological and basal autophagy [44].

We have shown in this study that MRT68921 can be a viable therapeutic tool for inhibiting ULK1 dependent autophagy induction in HGSOC spheroids. Although MRT68921 was first described to be highly specific towards ULK1 and ULK2, it also exhibited inhibitory activities to several other kinases such as NUAK1, IKKε, TBK1, and AMPK [28]. Therefore, our observation that MRT68921 caused significant cytotoxicity towards HGSOC spheroids may be a cumulative effect of inhibiting several oncogenic kinases, including ULK1. Recently two additional ULK inhibitors ULK-100 and ULK-101 were described, with ULK-100 being more potent [38]. It would be interesting to evaluate whether these ULK inhibitors have identical effects as MRT68921 on autophagy in HGSOC.

We believe that targeting ULK1 may be beneficial for improving treatment in HGSOC patients with metastatic disease. We found that high *ULK1* mRNA expression had a significant negative correlation with survival outcomes among advanced-stage serous ovarian cancer patients. This observation agrees to a recent finding that demonstrated a similar relationship between *ULK1* expression and survival [19], although the size of patient cohort used was smaller and did not focus on advanced-stage disease in which spheroid formation usually occurs.

In conclusion, we report that HGSOC spheroids have elevated ULK1 expression concomitant with autophagy induction. Indeed, HGSOC spheroids are sensitive to ULK1 kinase inhibition via MRT68921 treatment and fail to maintain viability in suspension culture, an important *in vitro* model of metastatic disease. Finally, since high expression of *ULK1* is a negative predictor of survival among advanced-stage serous ovarian cancer patients, we believe therapeutic targeting of ULK1 may hold promise for improving disease treatment.

Acknowledgements

This work was supported by the Ovarian Translational Research Initiative of the Ontario Institute for Cancer Research, the Cancer Research Society, Inc. in partnership with Ovarian Cancer Canada, and the London Run for Ovarian Cancer. We also thank our clinical colleagues for assisting with collection of patient ascites specimens, and special thanks to additional funding donors and ovarian cancer patients who have contributed to this research study.

Disclosure of conflict of interest

None.

Address correspondence to: Dr. Trevor G Shepherd, The Mary & John Knight Translational Ovarian Cancer Research Unit, London Regional Cancer Program, 790 Commissioners Rd. E., Room A4-836, London, Ontario, Room A4-836, London, ON N6A 4L6, Canada. E-mail: tshephe6@uwo.ca

References

[1] Burleson KM, Casey RC, Skubitz KM, Pambuccian SE, Oegema TR Jr and Skubitz AP. Ovarian carcinoma ascites spheroids adhere to extracellular matrix components and mesothelial cell monolayers. Gynecol Oncol 2004; 93: 170-181.

[2] Burleson KM, Hansen LK and Skubitz AP. Ovarian carcinoma spheroids disaggregate on type I collagen and invade live human mesothelial cell monolayers. Clin Exp Metastasis 2004; 21: 685-697.

[3] Iwanicki M, Davidowitz R, Ng M, Besser A, Muranen T, Merritt M, Danuser G, Ince T and Brugge J. Ovarian cancer spheroids use myosin-generated force to clear the mesothelium. Cancer Discov 2011; 1: 144-57.

[4] White E. Deconvoluting the context-dependent role for autophagy in cancer. Nat Rev Cancer 2012; 12: 401-10.

[5] Matthew R and White E. Autophagy in tumorigenesis and energy metabolism: friend by day, foe by night. Curr Opin Genet Dev 2011; 21: 113-119.

[6] Correa RJ, Valdes YR, Shepherd TG and DiMattia GE. Beclin-1 expression is retained in high-grade serous ovarian cancer yet is not essential for autophagy induction in vitro. J Ovarian Res 2015; 8: 52.

[7] Kim J, Kundu M, Viollet B and Guan KL. AMPK and mTOR regulate autophagy through direct phosphorylation of Ulk1. Nat Cell Biol 2011; 13: 132-141.

[8] Peart T, Ramos Valdes Y, Correa RJ, Fazio E, Bertrand M, McGee J, Préfontaine M, Sugimoto A, DiMattia GE and Shepherd TG. Intact LKB1 activity is required for survival of dormant ovarian cancer spheroids. Oncotarget 2015; 6: 22424-22438.

[9] Correa RJ, Peart T, Valdes YR, DiMattia GE and Shepherd TG. Modulation of AKT activity is associated with reversible dormancy in ascites-derived epithelial ovarian cancer spheroids. Carcinogenesis 2012; 33: 49-58.

[10] McAlpine F, Williamson LE, Tooze SA and Chan EY. Regulation of nutrient-sensitive autophagy by uncoordinated 51-like kinases 1 and 2. Autophagy 2013; 9: 361-373.

[11] Park JM, Jung CH, Seo M, Otto NM, Grunwald D, Kim KH, Moriarity B, Kim YM, Starker C, Nho RS, Voytas D and Kim DH. The ULK1 complex mediates MTORC1 signaling to the autophagy initiation machinery via binding and phosphorylating ATG14. Autophagy 2016; 12: 547-564.

[12] Nwadike C, Williamson LE, Gallagher LE, Guan JL and Chan EYW. AMPK inhibits ULK1-dependent autophagosome formation and lysosomal acidification via distinct mechanisms. Mol Cell Biol 2018; 38.

[13] Shang L, Chen S, Du F, Li S, Zhao L and Wang X. Nutrient starvation elicits an acute autophagic response mediated by Ulk1 dephosphorylation and its subsequent dissociation from AMPK. Proc Natl Acad Sci U S A 201122; 108: 4788-4793.

[14] Papinski D and Kraft C. Regulation of autophagy by signaling through the Atg1/ULK1 complex. J Mol Biol 2016; 428: 1725-1741.

[15] Cheong H, Lindsten T, Wu J, Lu C and Thompson CB. Ammonia-induced autophagy is independent of ULK1/ULK2 kinases. Proc Natl Acad Sci U S A 2011; 108: 11121-11126.

[16] Alers S, Löffler AS, Paasch F, Dieterle AM, Keppeler H, Lauber K, Campbell DG, Fehrenbacher B, Schaller M, Wesselborg S and Stork B. Atg13 and FIP200 act independently of Ulk1 and Ulk2 in autophagy induction. Autophagy 2011; 7: 1423-1433.

[17] Tamura N, Kageyama S, Komatsu M and Waguri S. Hyperosmotic stress induces uncon-

ventional autophagy independent of the Ulk1 complex. Mol Cell Biol 2019; 39: e00024-19.
[18] Corona Velazquez A, Corona AK, Klein KA and Jackson WT. Poliovirus induces autophagic signaling independent of the ULK1 complex. Autophagy 2018; 14: 1201-1213.
[19] Wheeler LJ, Watson ZL, Qamar L, Yamamoto TM, Sawyer BT, Sullivan KD, Khanal S, Joshi M, Ferchaud-Roucher V, Smith H, Vanderlinden LA, Brubaker SW, Caino CM, Kim H, Espinosa JM, Richer JK and Bitler BG. Multi-omic approaches identify metabolic and autophagy regulators important in ovarian cancer dissemination. iScience 2019; 19: 474-491.
[20] Wang B, Iyengar R, Li-Harms X, Joo JH, Wright C, Lavado A, Horner L, Yang M, Guan JL, Frase S, Green DR, Cao X and Kundu M. The autophagy-inducing kinases, ULK1 and ULK2, regulate axon guidance in the developing mouse forebrain via a noncanonical pathway. Autophagy 2018; 14: 796-811.
[21] Joo JH, Wang B, Frankel E, Ge L, Xu L, Iyengar R, Li-Harms X, Wright C, Shaw TI, Lindsten T, Green DR, Peng J, Hendershot LM, Kilic F, Sze JY, Audhya A and Kundu M. The noncanonical role of ULK/ATG1 in ER-to-Golgi trafficking is essential for cellular homeostasis. Mol Cell 2016; 62: 982.
[22] Li M, Lindblad JL, Perez E, Bergmann A and Fan Y. Autophagy-independent function of Atg1 for apoptosis-induced compensatory proliferation. BMC Biol 2016; 14: 70.
[23] Zachari M and Ganley IG. The mammalian ULK1 complex and autophagy initiation. Essays Biochem 2017; 61: 585-596.
[24] Hosokawa N, Hara T, Kaizuka T, Kishi C, Takamura A, Miura Y, Iemura S, Natsume T, Takehana K, Yamada N, Guan JL, Oshiro N and Mizushima N. Nutrient-dependent mTORC1 association with the ULK1-Atg13-FIP200 complex required for autophagy. Mol Biol Cell 2009; 20: 1981-1991.
[25] Nakaso K, Yoshimoto Y, Nakano T, Takeshima T, Fukuhara Y, Yasui K, Araga S, Yanagawa T, Ishii T and Nakashima K. Transcriptional activation of p62/A170/ZIP during the formation of the aggregates: possible mechanisms and the role in Lewy body formation in Parkinson's disease. Brain Res 2004; 1012: 42-51.
[26] He C and Klionsky DJ. Regulation mechanisms and signaling pathways of autophagy. Annu Rev Genet 2009; 43: 67-93.
[27] N'Diaye EN, Kajihara KK, Hsieh I, Morisaki H, Debnath J and Brown EJ. PLIC proteins or ubiquilins regulate autophagy-dependent cell survival during nutrient starvation. EMBO Rep 2009; 10: 173-179.
[28] Petherick KJ, Conway OJ, Mpamhanga C, Osborne SA, Kamal A, Saxty B and Ganley IG. Pharmacological inhibition of ULK1 kinase blocks mammalian target of rapamycin (mTOR)-dependent autophagy. J Biol Chem 2015; 290: 11376-11383.
[29] Pengo N, Agrotis A, Prak K, Jones J and Ketteler R. A reversible phospho-switch mediated by ULK1 regulates the activity of autophagy protease ATG4B. Nat Commun 2017; 8: 294.
[30] Gyorffy B, Lanczky A and Szallasi Z. Implementing an online tool for genome-wide validation of survival-associated biomarkers in ovarian-cancer using microarray data of 1287 patients. Endocr Relat Cancer 2012; 19: 197-208.
[31] Pagotto A, Pilotto G, Mazzoldi EL, Nicoletto MO, Frezzini S, Pastò A and Amadori A. Autophagy inhibition reduces chemoresistance and tumorigenic potential of human ovarian cancer stem cells. Cell Death Dis 2017; 8: e2943.
[32] Wang Q, Bu S, Xin D, Li B, Wang L and Lai D. Autophagy is indispensable for the self-renewal and quiescence of ovarian cancer spheroid cells with stem cell like properties. Oxid Med Cell Longev 2018; 2018: 7010472.
[33] Chen JL, David J, Cook-Spaeth D, Casey S, Cohen D, Selvendiran K, Bekaii-Saab T and Hays JL. Autophagy induction results in enhanced anoikis resistance in models of peritoneal disease. Mol Cancer Res 2017; 15: 26-34.
[34] Zachari M and Ganley IG. The mammalian ULK1 complex and autophagy initiation. Essays Biochem 2017; 61: 585-596.
[35] Kaizuka T and Mizushima N. Atg13 is essential for autophagy and cardiac development in mice. Mol Cell Biol 2015; 36: 585-95.
[36] Johnson CE and Tee AR. Exploiting cancer vulnerabilities: mTOR, autophagy, and homeostatic imbalance. Essays Biochem 2017; 61: 699-710.
[37] Egan DF, Chun MG, Vamos M, Zou H, Rong J, Miller CJ, Lou HJ, Raveendra-Panickar, D, Yang CC, Sheffler DJ, Teriete P, Asara JM, Turk BE, Cosford ND and Shaw RJ. Small molecule inhibition of the autophagy kinase ULK1 and identification of ULK1 substrates. Mol Cell 2015: 59; 285-297.
[38] Martin KR, Celano SL, Solitro AR, Gunaydin H, Scott M, O'Hagan RC, Shumway SD, Fuller P and MacKeigan JP. A potent and selective ULK1 inhibitor suppresses autophagy and sensitizes cancer cells to nutrient stress. iScience 2018; 8: 74-84.
[39] Li TY, Sun Y, Liang Y, Liu Q, Shi Y, Zhang CS, Zhang C, Song L, Zhang P, Zhang X, Li X, Chen T, Huang HY, He X, Wang Y, Wu YQ, Chen S, Ji-

ang M, Chen C, Xie C, Yang JY, Lin Y, Zhao S, Ye Z, Lin SY, Chiu DT and Lin SC. ULK1/2 constitute a bifurcate node controlling glucose metabolic fluxes in addition to autophagy. Mol Cell 2016; 62: 359-370.

[40] Lee E and Tournier C. The requirement of uncoordinated 51-like kinase 1 (ULK1) and ULK2 in the regulation of autophagy. Autophagy 2011; 7: 689-695.

[41] Kim YH, Baek SH, Kim EK, Ha JM, Jin SY, Lee HS, Ha HK, Song SH, Kim SJ, Shin HK, Yong J, Kim DH, Kim CD and Bae SS. Uncoordinated 51-like kinase 2 signaling pathway regulates epithelial-mesenchymal transition in A549 lung cancer cells. FEBS Lett 2016; 590: 1365-1374.

[42] Hieke N, Löffler AS, Kaizuka T, Berleth N, Böhler P, Drießen S, Stuhldreier F, Friesen O, Assani K, Schmitz K, Peter C, Diedrich B, Dengjel J, Holland P, Simonsen A, Wesselborg S, Mizushima N and Stork B. Expression of a ULK1/2 binding-deficient ATG13 variant can partially restore autophagic activity in ATG13-deficient cells. Autophagy 2015; 11: 1471-1483.

[43] Wang B and Kundu M. Canonical and noncanonical functions of ULK/Atg1. Curr Opin Cell Biol 2017; 45: 47-54.

[44] Chude CI and Amaravadi RK. Targeting autophagy in cancer: update on clinical trials and novel inhibitors. Int J Mol Sci 2017; 18: 1279.